

## Fractionation of Nb/Ta during subduction of carbonate-rich sediments

A. Bragagni, R. Avanzinelli, C. Münker, F. Mastroianni, S. Conticelli

### Supplementary Information

The Supplementary Information includes:

- Tyrrhenian Sea Samples Description
- Analytical Methods
- Quantifying the Role of Carbonate-rich Melts in Roman Magmatic Province
- Table S-1
- Figure S-1
- References for Literature Data in Figures 2 and 3
- Supplementary Information References

### Tyrrhenian Sea Samples Description

Samples from the Tyrrhenian basin were obtained from the MARUM GeoB Core Repository. They were originally collected during the Deep Sea Drilling Project (DSDP) and Ocean Drilling Program (ODP) in expedition 42 and 107. The samples were selected to be representative of the depleted magmatism recorded in the Tyrrhenian basin, which is thought to form in a back arc setting. In terms of composition they resemble that of transitional MORB and they are thought to derive from a depleted mantle slightly re-enriched by subduction-derived fluids (Barberi *et al.*, 1978; Beccaluva *et al.*, 1990; Dietrich *et al.*, 1977, 1978; Gasperini *et al.*, 2002; Hamelin *et al.*, 1979).

### Analytical Methods

Major element concentrations of the seven samples from the Tyrrhenian basin were obtained using a Philips PW 2400 XRF at the Universität zu Köln. The trace element content was determined following the procedure of Garbe-Schönberg (1993) and using an Agilent 7500cs ICP-MS at the Universität zu Kiel. The same samples were analysed for their Sr-Nd-Pb isotopic composition at the Università degli Studi di Firenze, leaching the powders in 1 M HCl and following the procedure described in Avanzinelli *et al.* (2005) for dissolution, chemical separation and TIMS measurements.

Elemental concentrations of HFSE (Nb, Ta, Zr, Hf), Lu, W, Th, and U were obtained along with  $^{176}\text{Hf}/^{177}\text{Hf}$  following the same procedure outlined in Bragagni *et al.* (2022), which is based on the methods described in Luo *et al.* (1997), Kirchenbaur *et al.* (2016), Münker *et al.* (2001), Münker (2010), Weyer *et al.* (2002), Kleine *et al.* (2004). Briefly, 100 mg of powder was weighted along with isotope tracers enriched in  $^{233-236}\text{U}$ – $^{229}\text{Th}$ – $^{183}\text{W}$ – $^{180}\text{Ta}$ – $^{180}\text{Hf}$ – $^{176}\text{Lu}$ – $^{94}\text{Zr}$ . Samples were dissolved and treated as described in Bragagni *et al.* (2022). Specifically, the W fraction was separated using anion resin exchange chemistry (modified from Kleine *et al.*, 2004), the HFSE were purified in three

steps of resin exchange chemistry (LN-spec, anion, LN-spec) using a modified procedure originally developed by Münker *et al.* (2001), U and Th were separated with TRU-spec chemistry (Luo *et al.*, 1997). All measurements were performed at Universität zu Köln with a Thermo-Scientific Neptune MC-ICP-MS equipped with a Cetac Aridus II. Blanks were 36–54 pg for W, 38–163 pg for Ta, 0.7–1.4 ng for Zr, 28–57 pg for Nb, 43–123 pg for Hf, 9 pg for Th and 35 pg for U, and are all negligible with respect to the amounts of sample processed.

## Quantifying the Role of Carbonate-rich Melts in Roman Magmatic Province

Quantifying the effect of silicate and carbonatitic melts in the investigated samples is not straightforward. This is due to the complexity of the involved processes and because melting parameters, such as partition coefficients, are not readily available. Green (2000) provides  $K_d$  for HFSE in rutile in equilibrium with carbonatitic magmas. However, in the case of marls, a silicate melt will also form along the carbonatite melt (*e.g.*, Gülmez *et al.*, 2023; Skora *et al.*, 2015). Therefore, to quantitatively model HFSE and other trace elements, both silicate and carbonatite partition coefficients must be considered. In the literature there are few experimental works reporting the trace element composition of melts in equilibrium with sediments at pressure and temperature relevant for mantle wedge conditions (Herman and Rubatto, 2009; Skora and Blundy, 2010; Skora *et al.*, 2015; Gülmez *et al.*, 2023). Among them, Skora *et al.* (2015) and Gülmez *et al.* (2023) investigated carbonate-rich lithologies but they do not report partition coefficients. The only experimental work with partition coefficients for sediments melt is Skora and Blundy (2010), which used a radiolarian clay lithology. These partition coefficients can be used to model melting of silicic sediments as those expected to influence the Tuscan magmatic province. Although not ideal, the same partition coefficient can be employed to reproduce the composition of a silicic melt in equilibrium with a marl, as needed to explain the Roman magmatism. As such, we assume that HFSE are controlled by rutile in equilibrium with a carbonatitic melt (partition coefficients of Green, 2000), whereas other elements are controlled by silicates in equilibrium with the silicic melt (partition coefficients of Skora and Blundy, 2010). It should be stressed that this is a simplification because also other elements can be influenced by carbonatite melts (especially REE). Moreover, also the partitioning of HFSE between rutile (and possibly other phases) and the silicate melt is not considered.

An alternative proxy of the metasomatic melt affecting the mantle wedge under the Roman magmatic province is represented by the carbonate-rich inclusions observed by Korsakov and Herman (2006) in orogenic massifs. Therefore, we model the effect of adding three different melts to a DMM, two inferred from melting silica- and carbonate-rich sediments, and one simply using the composition of a carbonate-rich inclusions of Korsakov and Herman (2006). Modelling was performed only with Nb/Ta and radiogenic isotope ratios to avoid variations of concentrations due to partial melting in the metasomatised mantle wedge. As shown in Figure S-1, mixing the DMM with silicic melt can reproduce the signature of the Tuscan magmatic province in Nb/Ta vs. Sr or Nd isotopes. The Roman magmas lie below the two mixing lines obtained for carbonate-rich metasomatic melts. This is readily explained by the concurrent occurrence of carbonate-rich metasomatic melts along with silicic melts (*i.e.* with canonical Nb/Ta) or fluids (*i.e.* negligible HFSE content but significant Sr and Nd).

## References for Literature Data in Figures 2 and 3

Reference values for PM values are taken from Münker *et al.* (2003) and Palme and O'Neill (2014). Literature isotope dilution data and Sr-Nd-Hf isotopes reported in Figure 3 are from: Tonga (Beier *et al.*, 2017), Cyprus (König *et al.*, 2008), Solomon (König *et al.*, 2008; Schuth *et al.*, 2009), Papua New Guinea (PNG) (König *et al.*, 2010), Kamchatka and Aleutian arc (Churikova *et al.*, 2001; Münker *et al.*, 2004; Yogodzinski *et al.*, 1995), Santorini and Bulgaria (Kirchenbaur *et al.*, 2012; Kirchenbaur and Münker, 2015), Sunda (Kirchenbaur *et al.*, 2022), Stromboli (Bragagni *et al.*, 2022).



## Supplementary Table

**Table S-1** Compiled dataset with HFSE concentrations measured by isotope dilution (this work and Bragagni *et al.*, 2022) along with major-trace elements and Hf-Sr-Nd-Pb isotope data (this work and indicated literature).

Table S-1 is available for download (.xlsx) from the online version of this article at <https://doi.org/10.7185/geochemlet.2410>.

## Supplementary Figure

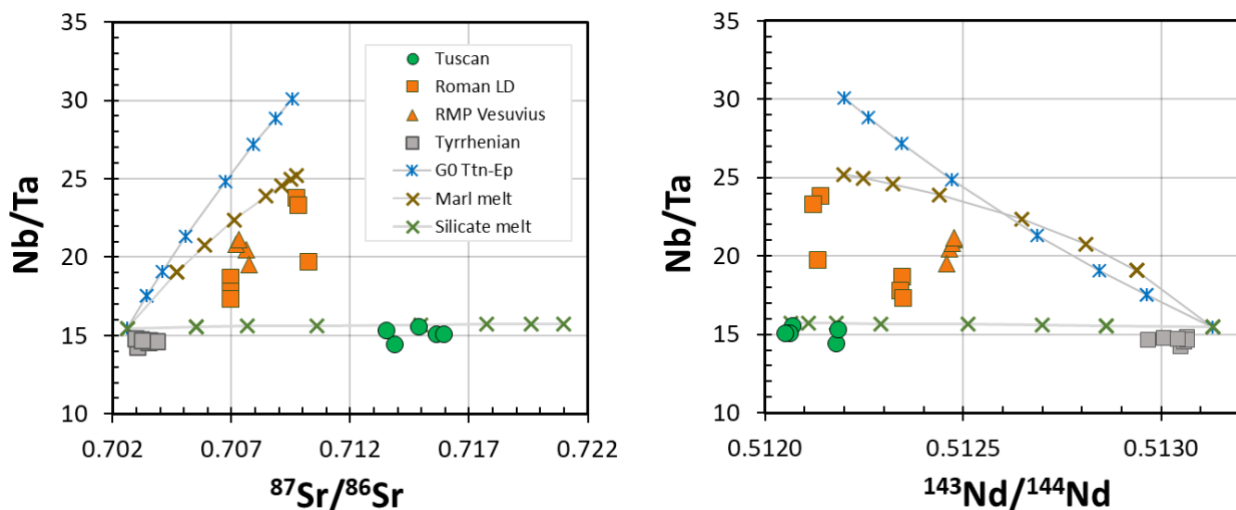


**Figure S-1** Mixing models to reproduce the Nb/Ta signature of the Roman and Tuscan magmatic provinces. The blue symbols represent a mixing curve between the DMM and the carbonate-rich melt (inclusion G0 Ttn-Ep) reported by Korsakov and Herman (2006) and assuming Sr and Nd isotope composition from marl SD53 (Casalini *et al.*, 2019). The brown and green crosses display a mixing between the DMM and melts from a carbonate-rich marl (SD53 of Conticelli, 1998; Conticelli *et al.*, 2015; Casalini *et al.*, 2019) or a carbonate poor lithology (SD75 of Conticelli, 1998; Conticelli *et al.*, 2015; Casalini *et al.*, 2019), respectively. For the marl melting, we assume that HFSE are controlled only by rutile, using the partition coefficients of Green (2020) for a carbonatitic melt and imposing a 1 % modal fraction of rutile. Partition coefficients for Sr and Nd are from Skora and Blundy (2010) (900 °C). We assume an arbitrary 50 % of partial melting of the marl. Such a melt was then mixed at variable proportions with the DMM. For melting the carbonate-poor lithology, we only used the partition coefficients of Skora and Blundy (2010) (900 °C) and assume a melting degree of 50 % before mixing it with the DMM. Symbols for the mixing models are reported adding 0, 0.5, 1, 2, 5, 10, 20, 50 % of sediment melt to the DMM. In a possible scenario, the Roman magmas are explained by the double contribution of melts from carbonate-rich (*i.e.* marl melting or G0 Ttn-Ep melt) and carbonate-poor lithologies (to lesser extent). Instead, the Tuscan magmas are explained by melting only the carbonate-poor lithology. DMM values are taken from Workman and Hart (2005).



## Supplementary Information References

- Avanzinelli, R., Boari, E., Conticelli, S., Francalanci, L., Guarnieri, L., Perini, G., Petrone, C.M., Tommasini, S., Ulivi, M. (2005) High precision Sr, Nd, and Pb isotopic analyses using the new generation Thermal Ionisation Mass Spectrometer ThermoFinnigan Triton-Ti®. *Periodico di Mineralogia* 74, 147–166. [https://flore.unifi.it/retrieve/e398c378-9905-179a-e053-3705fe0a4cff/2005PerMineral\\_Triton.pdf](https://flore.unifi.it/retrieve/e398c378-9905-179a-e053-3705fe0a4cff/2005PerMineral_Triton.pdf)
- Avanzinelli, R., Elliott, T., Tommasini, S., Conticelli, S. (2008) Constraints on the Genesis of Potassium-rich Italian Volcanic Rocks from U/Th Disequilibrium. *Journal of Petrology* 49, 195–223. <https://doi.org/10.1093/petrology/egm076>
- Avanzinelli, R., Braschi, E., Marchionni, S., Bindi, L. (2014) Mantle melting in within-plate continental settings: Sr–Nd–Pb and U-series isotope constraints in alkali basalts from the Sicily Channel (Pantelleria and Linosa Islands, Southern Italy). *Lithos* 188, 113–129. <https://doi.org/10.1016/j.lithos.2013.10.008>
- Avanzinelli, R., Casalini, M., Elliott, T., Conticelli, S. (2018) Carbon fluxes from subducted carbonates revealed by uranium excess at Mount Vesuvius, Italy. *Geology* 46, 259–262. <https://doi.org/10.1130/G39766.1>
- Barberi, F., Bizouard, H., Capaldi, G., Ferrara, G., Gasparini, P., Innocenti, F., Joron, J.L., Lambret, B., Treuil, M., Allegre, C. (1978) Age and nature of basalts from the Tyrrhenian abyssal plain. In: Hsu, K.J., Montadert, L., *et al.* (Eds.) *Initial Reports of the Deep Sea Drilling Project, Volume 42, Part 1*. U.S. Government Printing Office, Washington, D.C., 509–514. <http://doi.org/10.2973/dsdp.proc.42-1.118.1978>
- Beccaluva, L., Bonatti, E., Dupuy, C., Ferrara, G., Innocenti, F., Lucchini, F., Macera, P., Petrini, R., Rossi, P.L., Serri, G., Seyler, M., Siena, F. (1990) Geochemistry and mineralogy of volcanic rocks from ODP sites 650, 651, 655 and 654 in the Tyrrhenian Sea. In: Kastens, K.A., Mascle, J., *et al.* (Eds.) *Proceedings of the Ocean Drilling Program, Scientific Results, Volume 107*. Ocean Drilling Program, College Station, TX, 49–74. <http://doi.org/10.2973/odp.proc.sr.107.140.1990>
- Beier, C., Turner, S.P., Haase, K.M., Pearce, J.A., Münker, C., Regelous, M. (2017) Trace Element and Isotope Geochemistry of the Northern and Central Tongan Islands with an Emphasis on the Genesis of High Nb/Ta Signatures at the Northern Volcanoes of Tafahi and Niuatoputapu. *Journal of Petrology* 58, 1073–1106. <https://doi.org/10.1093/petrology/egx047>
- Boari, E., Tommasini, S., Laurenzi, M.A., Conticelli, S. (2009) Transition from Ultrapotassic Kamafugitic to Sub-alkaline Magmas: Sr, Nd, and Pb Isotope, Trace Element and <sup>40</sup>Ar–<sup>39</sup>Ar Age Data from the Middle Latin Valley Volcanic Field, Roman Magmatic Province, Central Italy. *Journal of Petrology* 50, 1327–1357. <https://doi.org/10.1093/petrology/egp003>
- Bouvier, A., Vervoort, J.D., Patchett, P.J. (2008) The Lu–Hf and Sm–Nd isotopic composition of CHUR: Constraints from unequilibrated chondrites and implications for the bulk composition of terrestrial planets. *Earth and Planetary Science Letters* 273, 48–57. <https://doi.org/10.1016/j.epsl.2008.06.010>
- Bragagni, A., Avanzinelli, R., Freymuth, H., Francalanci, L. (2014) Recycling of crystal mush-derived melts and short magma residence times revealed by U-series disequilibria at Stromboli volcano. *Earth and Planetary Science Letters* 404, 206–219. <https://doi.org/10.1016/j.epsl.2014.07.028>
- Bragagni, A., Mastroianni, F., Münker, C., Conticelli, S., Avanzinelli, R. (2022) A carbon-rich lithospheric mantle as a source for the large CO<sub>2</sub> emissions of Etna volcano (Italy). *Geology* 50, 486–490. <https://doi.org/10.1130/G49510.1>
- Casalini, M., Avanzinelli, R., Tommasini, S., Elliott, T., Conticelli, S. (2019) Ce/Mo and Molybdenum Isotope Systematics in Subduction-Related Orogenic Potassic Magmas of Central-Southern Italy. *Geochemistry, Geophysics, Geosystems* 20, 2753–2768. <https://doi.org/10.1029/2019GC008193>
- Conticelli, S. (1998) The effect of crustal contamination on ultrapotassic magmas with lamproitic affinity: mineralogical, geochemical and isotope data from the Torre Alfina lavas and xenoliths, Central Italy. *Chemical Geology* 149, 51–81. [https://doi.org/10.1016/S0009-2541\(98\)00038-2](https://doi.org/10.1016/S0009-2541(98)00038-2)



- Conticelli, S., Avanzinelli, R., Marchionni, S., Tommasini, S., Melluso, L. (2011) Sr-Nd-Pb isotopes from the Radicofani Volcano, Central Italy: constraints on heterogeneities in a veined mantle responsible for the shift from ultrapotassic shoshonite to basaltic andesite magmas in a post-collisional setting. *Mineralogy and Petrology* 103, 123–148. <https://doi.org/10.1007/s00710-011-0161-y>
- Conticelli, S., Avanzinelli, R., Ammannati, E., Casalini, M. (2015) The role of carbon from recycled sediments in the origin of ultrapotassic igneous rocks in the Central Mediterranean. *Lithos* 232, 174–196. <https://doi.org/10.1016/j.lithos.2015.07.002>
- Churikova, T., Dorendorf, F., Wörner, G. (2001) Sources and Fluids in the Mantle Wedge below Kamchatka, Evidence from Across-arc Geochemical Variation. *Journal of Petrology* 42, 1567–1593. <https://doi.org/10.1093/petrology/42.8.1567>
- Dietrich, V., Emmermann, R., Keller, J., Puchelt, H. (1977) Tholeiitic basalts from the Tyrrhenian Sea floor. *Earth and Planetary Science Letters* 36, 285–296. [https://doi.org/10.1016/0012-821X\(77\)90211-4](https://doi.org/10.1016/0012-821X(77)90211-4)
- Dietrich, V., Emmermann, R., Puchelt, H., Keller, J. (1978) Oceanic basalts from the Tyrrhenian basin, DSDP Leg 42A, Hole 373A. In: Hsu, K.J., Montadert, L., et al. (Eds.) *Initial Reports of the Deep Sea Drilling Project, Volume 42, Part 1*. U.S. Government Printing Office, Washington, D.C., 515–530. <https://doi.org/10.2973/dsdp.proc.42-1.119.1978>
- Garbe-Schönberg, C.-D. (1993) Simultaneous Determination of Thirty-Seven Trace Elements in Twenty-Eight International Rock Standards by ICP-MS. *Geostandards Newsletter* 17, 81–97. <https://doi.org/10.1111/j.1751-908X.1993.tb00122.x>
- Gasperini, D., Blichert-Toft, J., Bosch, D., Del Moro, A., Macera, P., Albarède, F. (2002) Upwelling of deep mantle material through a plate window: Evidence from the geochemistry of Italian basaltic volcanics. *Journal of Geophysical Research: Solid Earth* 107, 2367. <https://doi.org/10.1029/2001JB000418>
- Green, T.H. (2000) New partition coefficient determinations pertinent to hydrous melting processes in subduction zones. In: Smith, I.E.M., Davidson, J.P., Gamble, J.A., Price, R.C. (Eds.) *Processes and Time Scales in the Genesis and Evolution of ARC Magmas*. Royal Society of New Zealand, Wellington, 92–95.
- Gülmez, F., Prelević, D., Förster, M.W., Buhre, S., Günther, J. (2023) Experimental production of K-rich metasomes through sediment recycling at the slab-mantle interface in the fore-arc. *Scientific Reports* 13, 19608. <https://doi.org/10.1038/s41598-023-46367-7>
- Hamelin, B., Lambret, B., Joron, J.-L., Treuil, M., Allègre, C.J. (1979) Geochemistry of basalts from the Tyrrhenian Sea. *Nature* 278, 832–834. <https://doi.org/10.1038/278832a0>
- Hermann, J., Rubatto, D. (2009) Accessory phase control on the trace element signature of sediment melts in subduction zones. *Chemical Geology* 265, 512–526. <https://doi.org/10.1016/j.chemgeo.2009.05.018>
- Kirchenbaur, M., Münker, C. (2015) The behaviour of the extended HFSE group (Nb, Ta, Zr, Hf, W, Mo) during the petrogenesis of mafic K-rich lavas: The Eastern Mediterranean case. *Geochimica et Cosmochimica Acta* 165, 178–199. <https://doi.org/10.1016/j.gca.2015.05.030>
- Kirchenbaur, M., Münker, C., Schuth, S., Garbe-Schönberg, D., Marchev, P. (2012) Tectonomagmatic Constraints on the Sources of Eastern Mediterranean K-rich Lavas. *Journal of Petrology* 53, 27–65. <https://doi.org/10.1093/petrology/egr055>
- Kirchenbaur, M., Maas, R., Ehrig, K., Kamenetsky, V.S., Strub, E., Ballhaus, C., Münker, C. (2016) Uranium and Sm isotope studies of the supergiant Olympic Dam Cu–Au–U–Ag deposit, South Australia. *Geochimica et Cosmochimica Acta* 180, 15–32. <https://doi.org/10.1016/j.gca.2016.01.035>
- Kirchenbaur, M., Schuth, S., Barth, A.R., Luguët, A., König, S., Idrus, A., Garbe-Schönberg, D., Münker, C. (2022) Sub-arc mantle enrichment in the Sunda rear-arc inferred from HFSE systematics in high-K lavas from Java. *Contributions to Mineralogy and Petrology* 177, 8. <https://doi.org/10.1007/s00410-021-01871-9>



- Kleine, T., Mezger, K., Münker, C., Palme, H., Bischoff, A. (2004)  $^{182}\text{Hf}$ - $^{182}\text{W}$  isotope systematics of chondrites, eucrites, and martian meteorites: Chronology of core formation and early mantle differentiation in Vesta and Mars. *Geochimica et Cosmochimica Acta* 68, 2935–2946. <https://doi.org/10.1016/j.gca.2004.01.009>
- König, S., Münker, C., Schuth, S., Garbe-Schönberg, D. (2008) Mobility of tungsten in subduction zones. *Earth and Planetary Science Letters* 274, 82–92. <https://doi.org/10.1016/j.epsl.2008.07.002>
- König, S., Münker, C., Schuth, S., Luguet, A., Hoffmann, J.E., Kuduon, J. (2010) Boninites as windows into trace element mobility in subduction zones. *Geochimica et Cosmochimica Acta* 74, 684–704. <https://doi.org/10.1016/j.gca.2009.10.011>
- Korsakov, A.V., Hermann, J. (2006) Silicate and carbonate melt inclusions associated with diamonds in deeply subducted carbonate rocks. *Earth and Planetary Science Letters* 241, 104–118. <https://doi.org/10.1016/j.epsl.2005.10.037>
- Luo, X., Rehkämper, M., Lee, D.-C., Halliday, A.N. (1997) High precision  $^{230}\text{Th}/^{232}\text{Th}$  and  $^{234}\text{U}/^{238}\text{U}$  measurements using energyfiltered ICP magnetic sector multiple collector mass spectrometry. *International Journal of Mass Spectrometry and Ion Processes* 171, 105–117. [https://doi.org/10.1016/S0168-1176\(97\)00136-5](https://doi.org/10.1016/S0168-1176(97)00136-5)
- Münker, C. (2010) A high field strength element perspective on early lunar differentiation. *Geochimica et Cosmochimica Acta* 74, 7340–7361. <https://doi.org/10.1016/j.gca.2010.09.021>
- Münker, C., Weyer, S., Scherer, E., Mezger, K. (2001) Separation of high field strength elements (Nb, Ta, Zr, Hf) and Lu from rock samples for MC-ICPMS measurements. *Geochemistry, Geophysics, Geosystems* 2, 2001GC000183. <https://doi.org/10.1029/2001GC000183>
- Münker, C., Pfänder, J.A., Weyer, S., Büchl, A., Kleine, T., Mezger, K. (2003) Evolution of Planetary Cores and the Earth-Moon System from Nb/Ta Systematics. *Science* 301, 84–87. <https://doi.org/10.1126/science.1084662>
- Münker, C., Wörner, G., Yogodzinski, G., Churikova, T. (2004) Behaviour of high field strength elements in subduction zones: constraints from Kamchatka–Aleutian arc lavas. *Earth and Planetary Science Letters* 224, 275–293. <https://doi.org/10.1016/j.epsl.2004.05.030>
- Palme, H., O'Neill, H.St.C. (2014) 3.1 - Cosmochemical Estimates of Mantle Composition. In: Holland, H.D., Turekian, K.K. (Eds.) *Treatise on Geochemistry*. Second Edition, Elsevier, Oxford, 1–39. <https://doi.org/10.1016/B978-0-08-095975-7.00201-1>
- Schuth, S., Münker, C., König, S., Qopoto, C., Basi, S., Garbe-Schönberg, D., Ballhaus, C. (2009) Petrogenesis of Lavas along the Solomon Island Arc, SW Pacific: Coupling of Compositional Variations and Subduction Zone Geometry. *Journal of Petrology* 50, 781–811. <https://doi.org/10.1093/petrology/egp019>
- Skora, S., Blundy, J. (2010) High-pressure Hydrous Phase Relations of Radiolarian Clay and Implications for the Involvement of Subducted Sediment in Arc Magmatism. *Journal of Petrology* 51, 2211–2243. <https://doi.org/10.1093/petrology/egq054>
- Skora, S., Blundy, J.D., Brooker, R.A., Green, E.C.R., de Hoog, J.C.M., Connolly, J.A.D. (2015) Hydrous Phase Relations and Trace Element Partitioning Behaviour in Calcareous Sediments at Subduction-Zone Conditions. *Journal of Petrology* 56, 953–980. <https://doi.org/10.1093/petrology/egv024>
- Tommasini, S., Heumann, A., Avanzinelli, R., Francalanci, L. (2007) The Fate of High-Angle Dipping Slabs in the Subduction Factory: an Integrated Trace Element and Radiogenic Isotope (U, Th, Sr, Nd, Pb) Study of Stromboli Volcano, Aeolian Arc, Italy. *Journal of Petrology* 48, 2407–2430. <https://doi.org/10.1093/petrology/egm066>
- Weyer, S., Münker, C., Rehkämper, M., Mezger, K. (2002) Determination of ultra-low Nb, Ta, Zr and Hf concentrations and the chondritic Zr/Hf and Nb/Ta ratios by isotope dilution analyses with multiple collector ICP-MS. *Chemical Geology* 187, 295–313. [https://doi.org/10.1016/S0009-2541\(02\)00129-8](https://doi.org/10.1016/S0009-2541(02)00129-8)



Yogodzinski, G.M., Kay, R.W., Volynets, O.N., Koloskov, A.V., Kay, S.M. (1995) Magnesian andesite in the western Aleutian Komandorsky region: Implications for slab melting and processes in the mantle wedge. *GSA Bulletin* 107, 505–519. [https://doi.org/10.1130/0016-7606\(1995\)107<0505:MAITWA>2.3.CO;2](https://doi.org/10.1130/0016-7606(1995)107<0505:MAITWA>2.3.CO;2)

Workman, R.K., Hart, S.R. (2005) Major and trace element composition of the depleted MORB mantle (DMM). *Earth and Planetary Science Letters* 231, 53–72. <https://doi.org/10.1016/j.epsl.2004.12.005>

